Doctoral Forum on Vacuum Electronics (FVE 2017)

22–23 August 2017

# Design of a 340 GHz phase-velocity-taper travelling wave tube

*Wei Shao[1], Qing Zhou[1], Hanwen Tian[1], Xianbao Shi[1], Zhanliang Wang[1], Yanyu Wei[1], Zhaoyun Duan[1], Yubin Gong[1], Jinjun Feng[2]*

[1]*National Key Laboratory of Science and Technology on Vacuum Electronics, University of Electronic Science and Technology of China, No.4, Section 2, North Jianshe Road, Chengdu, People's Republic of China*
[2]*Beijing Vacuum Electronics Research Institute, No.13, Jiuxianqiao Road, Beijing, People's Republic of China*
*E-mail: ybgong@uestc.edu.cn*

Published in *The Journal of Engineering*; Received on 8th February 2018; Accepted on 17th April 2018

**Abstract:** Staggered double-vane slow wave structure as the core part of the travelling wave tube (TWT) has been more popular in recent years. However, the electron efficiency of this structure is not enough high for higher frequency, especially THz. In this study, phase-velocity-taper method is utilised for the improvement of TWT's efficiency at 340 GHz. The reflection and transmission coefficients of the whole tube with attenuator show good propagation characteristics over the wide frequency range from 330 to 345 GHz. The particle-in-cell simulation results indicate that the output power can increase about 32% at 340 GHz with respect to that of the without-taper structure. The corresponding electron efficiency is improved from 2.8 to 3.5% by phase-velocity-taper. However, the simulation results also show that the tube can produce over 30 W output power in the frequency range from 330 to 343 GHz with an operating voltage of 21.3 kV, a current of 0.043 A, and an input power of 10 mW. In addition, a sheet beam electron gun with a beam current of 43 mA, a beam voltage of 21.3 kV, and beam waist cross-sectional dimension of 0.3 mm × 0.08 mm is also designed as the particle source of the sheet-beam TWT.

## 1 Introduction

Terahertz wave, which is defined as frequencies from 100 GHz to 10 THz, has significant impacts on improving the performance of modern applications such as security, biomedical imaging, and radar systems [1–5]. Relevant to this topic, there are some devices that can generate terahertz radiation, such as free electron lasers, travelling wave tubes (TWTs) and backward wave oscillators (BWOs). Among these devices, TWTs have attracted considerable interests for their high efficiency of energy conversion and thermal capacity.

Due to that, the performance of slow-wave structures (SWSs) are closely linked to the whole tube's performance, the SWSs have attracted a lot of interests in recent years. The most popular SWS in THz wave band is folded waveguide [6–8] which can provide a wider bandwidth and higher output power. However, the circular beam tunnel in the waveguide makes the microfabrication processes difficult. In contrast, it's relatively easy to fabricate for rectangular SWS due to its normal sheet beam tunnels, such as sine waveguide, trapezoidal corrugated waveguide, and staggered double vane [9–11]. Mineo and Paoloni reported a G-band double-corrugated TWT with output power up to 3.7 W, 18 dB gain in the frequency range of 210–240 GHz [12]. Shin *et al.* have proposed a novel terahertz sheet-beam TWT amplifier which can produce above 150–250 W output power, corresponding to ~3–5.5% intrinsic electronic efficiency and over 25% bandwidth at the centre frequency of 220 GHz [13–17].

In addition, the geometry of sheet beam allows a larger beam current compared with the traditional circular beam. With the same current, a lower beam current density can be obtained with sheet beam which can reduce the space-charge effect and increase the perveance. Therefore, the rectangular SWSs which utilise sheet beam have been more popular among TWTs.

However, the decrease of TWT's energy conversion efficiency with the increasing frequency has been a seriously important problem. Particularly, there is a shortage that the beam energy cannot get a valid conversion in the second section of TWT and the energy is wasted mostly. One approach to the problem is to utilise the phase-velocity-taper method [17, 18]. In principle, the velocity of the beam will resynchronise with the phase velocity by tapering a circuit wavelength (periodic length) at the TWT's second section.

In this paper, a 340 GHz sheet-beam phase-velocity-taper staggered double-vane TWT is proposed with a good amplification performance. The geometric parameters and the mechanism of phase-velocity-taper are shown in Section 2. The result of the beam-wave interaction is mentioned in Section 3. And Section 3 also illustrates the comparison of the structures with/without tapered. Based on these, a sheet beam electron gun is designed at Section 4. Finally, some conclusions are drawn in Section 5.

## 2 Transmission characteristics

The three-dimensional (3D) model and the geometric parameters of the normal staggered double-vane slow wave structure (SWS) [11, 18] are shown in Fig. 1. The vane width, height, and thickness are $w$, $h$, $g$, respectively, and the vane period is $p$. All the parameters are shown in Table 1 and Fig. 2 shows the phase velocity versus frequency with respect to different period lengths. It can be seen that with the reduce of period length from 0.432 to 0.428 mm, the normalised phase velocity of SWS is decreased a little and the curves with different period lengths show a good flatness among a wide frequency range.

The whole tapered tube including the SWS, the rectangular attenuator and the ridge-loaded waveguide input/output coupler is shown in Fig. 3. The periods of the first and the second sections of the TWT are 45 and 120, respectively. For the staggered double-vane SWS, a well-designed input/output coupler can greatly restrain the signal reflection and the self-oscillation. Shin *et al.* have proposed a good coupler for their sheet-beam TWT [19, 20], but the


doi: 10.1049/joe.2018.0110

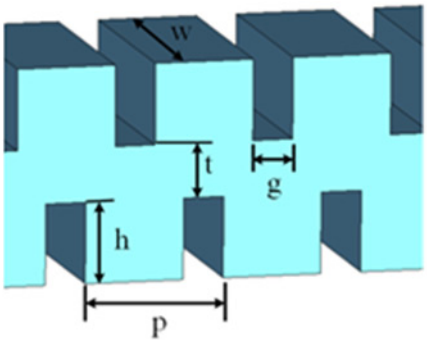


**Fig. 1** *3D vacuum model of the staggered double-vane SWS*

**Table 1** Design dimensions of the single period of the SWS

| Parameters | Dimension, mm |
|---|---|
| *w* | 0.34 |
| *h* | 0.12 |
| *g* | 0.15 |
| *p* | 0.43 |
| *t* | 0.12 |

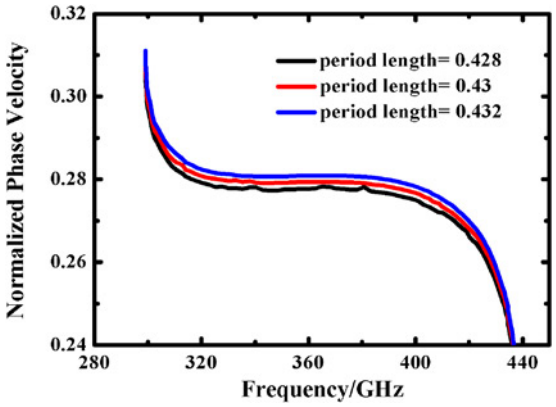


**Fig. 2** *Normalised phase velocity of the staggered double-vane SWS*

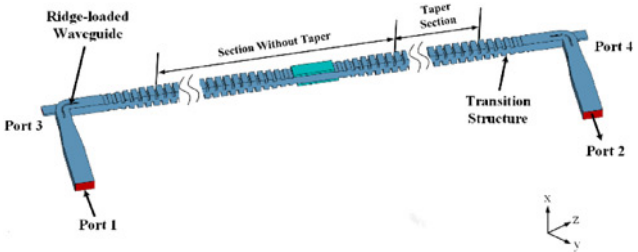


**Fig. 3** *3D model of the whole tapered tube with attenuator*

structure is complex relatively for the fabrication. In this paper, a suitable input/output coupler for this structure is designed according to the method proposed by Lai *et al.* [11] and it is composed of two parts: transition structure and input/output connector. Moreover, to prevent the reflection wave oscillations caused by the coupler and the impedance mismatch of the RF structure, a concentrated attenuator is designed [18, 21] in this paper. The attenuator's position where is inserted in the SWS can be inferred from the criterion equation [11, 22]

$$Q = G - L - \Gamma_{\text{out}} - \Gamma_{\text{in}}$$

where $G$ is the gain of the TWT, $L$ is the circuit loss, $\Gamma_{\text{out}}$ and $\Gamma_{\text{in}}$ are the reflection coefficients of output and input ports, respectively. All parameters are expressed in decibel. Considering that the tube will oscillate when $Q > 0$, the attenuator is inserted at the 45 periods of the SWS and included 5 periods, which is shown in Fig. 3. *CP-BeO* (Carburized porous beryllium oxide) with a loss tangent of 0.5 and relative permittivity of 6.5 is selected for the attenuator.

The taper section is located in the second section of the TWT [21]. The tapered period length and tapered period number of the velocity-tapered structures are shown in Fig. 4. The one-step taper design is selected in this paper and the tapered period of 0.428 mm begins from the 70th period to the end of the second section. The lower left in Fig. 4 inset shows the normalised phase velocity compared with different period length. It is observed that the phase velocity is very nearly the same as the result without taper. It means that the change of period length has a negligible effect on the operating bandwidth of the tube.

As shown in Fig. 5, the reflection coefficient $(S_{11})$ is less than −18 dB over the frequency range from 330 to 345 GHz. And the transmission coefficient $(S_{21})$ with attenuator shows a good absorption capacity. The curves $S_{31}$ and $S_{41}$ also indicate that the electromagnetic wave cannot propagate through the ports of beam tunnel.

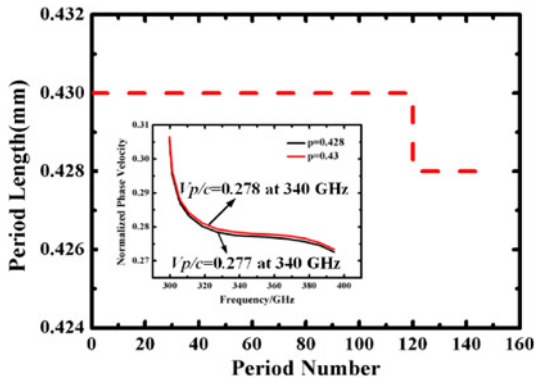


**Fig. 4** *Parameters of the velocity-tapered structure*

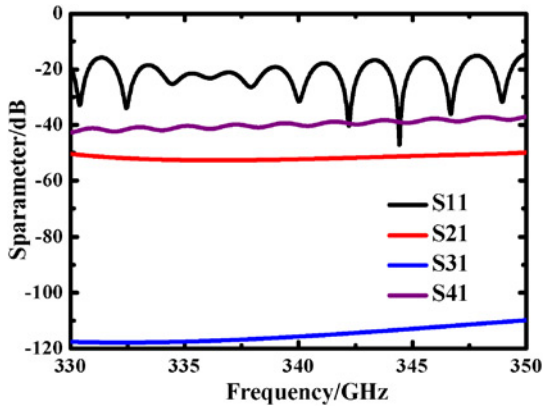


**Fig. 5** *S-parameters of the model with attenuator*

## 3 Beam–wave interaction

Considering the space-charge effect, the beam current is optimised based on the cross-section of the beam and the current density is 200 A/cm$^2$. The operating voltage is selected as 21.3 kV and the continuous wave excitation signal of 10 mW input power is applied in the simulation. Fig. 6 shows the power of output signal at 340 GHz. A stable output signal is obtained after 1 ns with 32 W output power and 35 dB gain. It also can be seen that the output power at 340 GHz has increased about 32% compared with the without-taper structure. The corresponding electron efficiency is improved from 2.8 to 3.5% by phase-velocity-taper. In terms of the basic theory, the energy conversion and power amplification can be continued by tapering the phase velocity. The slowed electron that loses the kinetic energy can be further synchronised with the wave so that obtain higher output power [21].

Figs. 7 and 8 show the beam energy distribution along the longitudinal direction of the circuit without/with taper, respectively. As the beam moves along the longitudinal direction, the continuous beam–wave interaction leads to the decrease of electron velocity. Based on this, non-synchronisation is forming between the beam and the wave at the second section of the tube. The phase velocity tapering method can help to enhance the overall beam–wave interaction [17, 21]. It's noted that the beam energy transfers more 300 eV energy to the wave by the velocity-taper compared with the without-taper result.

In order to predict the instantaneous bandwidth of the TWT, the simulations are calculated at discrete frequency points over the passband. The results of the output power versus the frequency are shown in Fig. 9. As can be seen, the power reaches over 30 W in the frequency range from 330 to 343 GHz, and the maximum output power reaches 34.7 W at 336 GHz, which corresponds to a gain of 35.4 dB. It can be observed that the maximum output power has a frequency shift compared with the structure without taper, which is due to the fact that the optimum voltage of taper section is not mismatched with the initial operating voltage. The output power drops in the lower and upper cut-off frequencies are due to the synchronous condition is broken. As it can

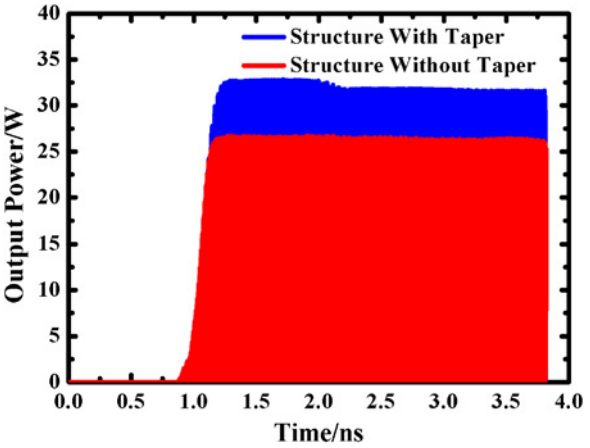


**Fig. 6** *Output power of the velocity-tapered tube compared with the without-taper structure*

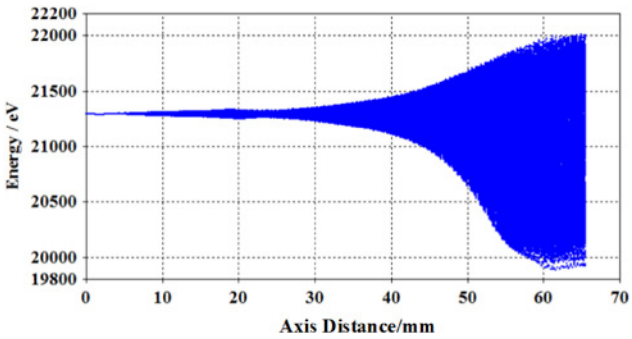


**Fig. 7** *Beam energy distribution of the structure without taper*

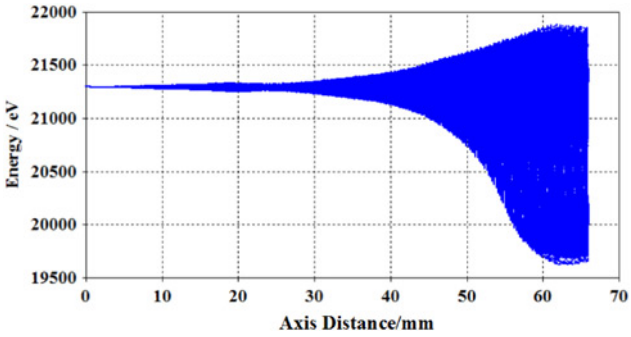


**Fig. 8** *Beam energy distribution of the taper structure*

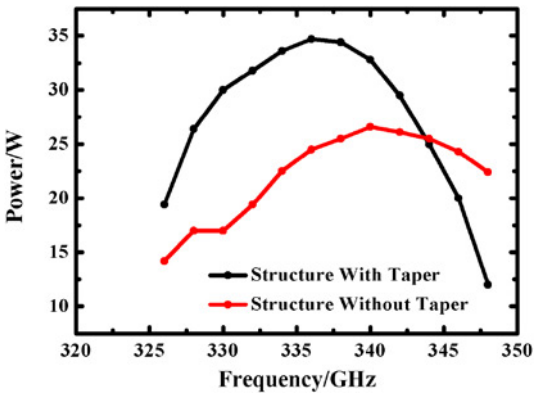


**Fig. 9** *Results of the output power versus frequency compared with the without-taper structure*

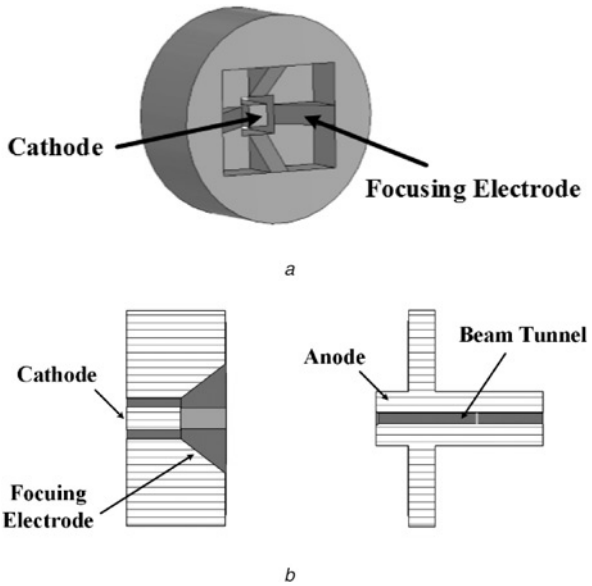


**Fig. 10** *Sketch of the electron gun*
*a* Cathode and focusing electrode
*b* Cross-sectional view of the gun

be seen, the power amplification is obviously enhanced over the wide bandwidth by tapering the phase-velocity of the circuit.

## 4 Design of sheet-beam electron gun

In general, there are two methods can be used for generating sheet electron beam. One method is compressing the circular electron beam into a sheet electron beam by the magnetic field, which also is called a high elliptical electron beam [18, 23]. The other is compressing the sheet electron beam directly. In this paper, the latter is used and the sketch of the electron gun is shown in Fig. 10. Here, the voltage of the cathode and the focusing electrode is set as −21.3 kV and the anode is zero relatively.

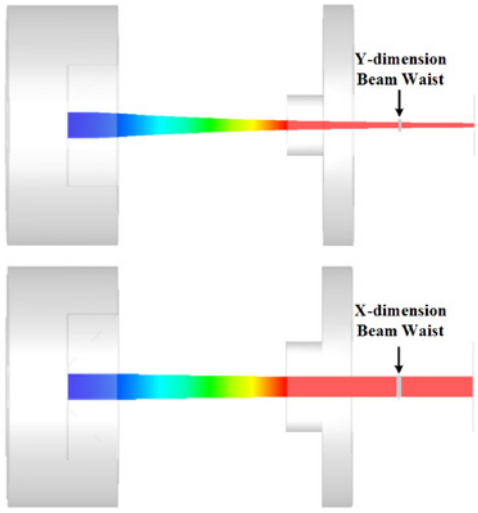


**Fig. 11** *Electron beam in the X-direction and Y-direction*

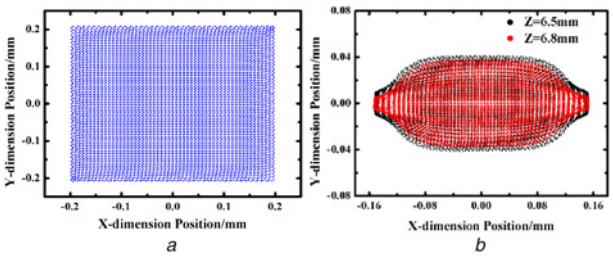


**Fig. 12** *2D particle distribution at the cross-sectional planes*
*a* At cathode surface
*b* At $Z = 6.5$ and 6.8 mm

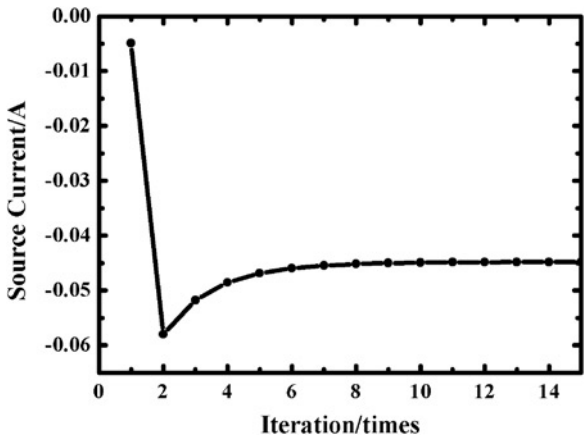


**Fig. 13** *Cathode emission current of the gun*

A rectangular emission surface of 0.4 mm × 0.42 mm is applied and the electron beam is compressed in the $X$ and $Y$ directions, respectively. As shown in Fig. 11, the beam waists in the $X$-direction and the $Y$-direction are closely at the same $Z$-position.

Fig. 12 shows the 2D particle distribution at the cross-sectional planes: Fig. 12*a* at the cathode surface and Fig. 12*b* at the $Z = 6.5$ and 6.8 mm. The electron beam is compressed in the $X$-direction and the $Y$-direction with different ratios and the comparison of different positions in Fig. 12*b* indicates that there is no obvious compression in the $X$-direction. The cathode emission current is converged to 43 mA with more than ten iterations, which is shown in Fig. 13. With these, a sheet-beam electron gun with a beam current of 43 mA, a beam voltage of 21.3 kV, and cross-sectional dimension of 0.3 mm × 0.08 mm is obtained.

## 5 Conclusion

A 340 GHz phase-velocity-taper staggered double-vane TWT is studied in this paper. The beam–wave interaction shows that the TWT can obtain a gain of >34.7 dB in the frequency range from 330 to 343 GHz. However, the output power can be increased about 32% at 340 GHz with the one-step velocity-tapered method. Obviously, an enhanced interaction has been obtained by employing this method. A sheet-beam electron gun with a beam current of 43 mA, a beam voltage of 21.3 kV, and cross-sectional dimension of 0.3 mm × 0.08 mm is also obtained. Based on the simulation results, the manufacture and test will be carried out in the near future.

## 6 Acknowledgments

This work was supported by the National Science Foundation of China (grant no. 61531010).

## 7 References

[1] Borsuk G.M., Levush B.: 'Vacuum electronics research perspective at the naval research laboratory'. IEEE Int. Vacuum Electron. Conf., Monterey, USA, 21–24 May, 2010, p. 3
[2] Booske J.H.: 'Plasma physics and related challenges of millimeter-wave-to-terahertz and high power microwave generation', *Phys. Plasmas*, 2008, **15**, (5), pp. 055502-1–055502-16
[3] Gee A., Shin Y.-M.: 'Gain analysis of higher-order-mode amplification in a dielectric-implanted multi-beam traveling wave structure', *Phys. Plasmas*, 2013, **20**, p. 073106
[4] Tucek J., Basten M., Gallagher D., *ET AL.*: 'Sub-millimeter and THz power amplifier development at Northrop Grumman'. IEEE Int. Vacuum Electronics Conf., Monterey, USA, 21–24 May, 2010, p. 19
[5] Shin Y.-M, Barnett L.R, Luhmann N.C.: 'Strongly confined plasmonic wave propagation through an ultrawideband staggered double grating waveguide', *Appl. Phys. Lett.*, 2008, **93**, p. 221504
[6] Cai J., Feng J., Hu Y., *ET AL.*: '10 GHz bandwidth 100 W W-band folded waveguide pulsed TWTs', *IEEE Microw. Wireless Compon. Lett.*, 2014, **24**, (9), pp. 620–621
[7] Wei Y., Guo G., Gong Y., *ET AL.*: 'Novel W-band ridge-loaded folded waveguide traveling wave tube', *IEEE Electron Device Lett.*, 2014, **35**, (10), pp. 1058–1060
[8] Bhattacharjee S., Booske J.H., Kory C.L., *ET AL.*: 'Folded waveguide traveling-wave tube sources for terahertz radiation', *IEEE Trans. Plasma Sci.*, 2003, **32**, (3), pp. 1002–1014
[9] Xiong X., Wei Y., Fei S., *ET AL.*: 'Research of sine waveguide slow-wave structure for a 220-GHz backward wave oscillator', *Chin. Phys. B*, 2012, **21**, p. 068402
[10] Xu X., Wei Y.Y., Shen F., *ET AL.*: 'Sine waveguide for 0.22-THz traveling-wave tube', *IEEE Trans. Electron Devices*, 2011, **32**, (8), pp. 1152–1154
[11] Lai J., Wei Y., Gong Y., *ET AL.*: 'W-band 1-kW staggered double-vane traveling-wave tube', *IEEE Trans. Electron Devices*, 2012, **59**, (2), pp. 496–503
[12] Mineo M., Paoloni C.: 'Double-corrugated rectangular waveguide slow-wave structure for terahertz vacuum devices', *IEEE Trans. Electron Devices*, 2012, **59**, (2), pp. 3169–3175

[13] Shin Y.-M., Baig A., Barnett L.R, *ET AL.*: 'System design analysis of a 0.22-THz sheet-beam traveling-wave tube amplifier', *IEEE Trans. Electron Devices*, 2012, **59**, (1), pp. 234–240
[14] Shin Y.-M., Barnett L.R.: 'Intense wideband terahertz amplification using phase shifted periodic electron-plasmon coupling', *Appl. Phys. Lett.*, 2008, **92**, (9), pp. 091501-1–091501-3
[15] Shin Y.-M, Baig A, Barnett L.R, *ET AL.*: 'Modeling investigation of an ultrawideband terahertz sheet beam traveling-wave tube amplifier circuit', *IEEE Trans. Electron Devices*, 2011, **58**, (9), pp. 3213–3218
[16] Shin Y.M., Barnett L.R., Luhmann N.C.: 'Phase-shifted traveling-wave-tube circuit for ultrawideband high-power submillimeter-wave generation', *IEEE Trans. Electron Devices.*, 2009, **56**, (5), pp. 706–712
[17] Palm A., Sirigiri J., Shin Y.-M.: 'Enhanced traveling wave amplification of co-planar slow wave structure by extended phase-matching', *Phys. Plasmas.*, 2015, **22**, p. 093121
[18] Shi X., Wang Z., Tang X., *ET AL.*: 'Study on wideband sheet beam traveling wave tube based on staggered double vane slow wave structure', *IEEE Trans. Plasma Sci.*, 2014, **42**, (12), pp. 3996–4003
[19] Carlsten B.E., Russell S.J., Earley L.M., *ET AL.*: 'Technology development for an mm-wave sheet-beam traveling-wave tube', *IEEE trans. Plasma Sci.*, 2005, **33**, (1), pp. 85–93
[20] Shin Y.-M., Barnett L.R., Baig A., *ET AL.*: '0.22 THz sheet beam TWT amplifier: system design and analysis'. IEEE Int. Vacuum Electronics Conf., Bangalore, India, 2011, pp. 61–62
[21] Shi X., Billa L.R., Gong Y., *ET AL.*: 'High efficiency and high power staggered double vane TWT amplifier enhanced by velocity-taper design', *Progress Electromagn. Res. C*, 2016, **66**, (5), pp. 39–46
[22] Gilmour A.S.: 'Principles of traveling-wave tubes' (Artech House, Boston, MA, 1994)
[23] Liu H., Wang Z., Gong Y., *ET AL.*: 'Study on Ka-band sheet-beam, three-slot-staggered-ladder coupled-cavity traveling-wave tube in a small tunable periodic cusped magnet', *J. Electromagn. Waves Appl.*, 2017, **31**, pp. 1924–1937